*galaxies*

MDPI

*Article*

# Millimeter VLBI of NGC 1052: Dynamics

**Anne-Kathrin Baczko [1,2,3,*], Robert Schulz [1,2,4], Eduardo Ros [3,5], Matthias Kadler [2], Manel Perucho [5] and Jörn Wilms [1]**

1 Dr. Remeis-Sternwarte & ECAP, University Erlangen-Nürnberg, Sternwartstr. 7, 96049 Bamberg, Germany; schulz@astron.nl (R.S.); joern.wilms@sternwarte.uni-erlangen.de (J.W.)
2 Institut für Th. Physik und Astrophysik, University Würzburg, Emil-Fischer-Str. 31, 97074 Würzburg, Germany; matthias.kadler@astro.uni-wuerzburg.de
3 Max-Planck-Institut für Radioastronomie, Auf dem Hügel 69, 53121 Bonn, Germany; ros@mpifr-bonn.mpg.de
4 Netherlands Institute for Radio Astronomy (ASTRON), PO Box 2, 7990 AA Dwingeloo, The Netherlands
5 Obs. Astronòmic & Department d'As. i Astr., University de València, E-46071 València, Spain; manel.perucho@uv.es
* Correspondence: baczko@mpifr-bonn.mpg.de

Academic Editors: Jose L. Gómez, Alan P. Marscher and Svetlana G. Jorstad
Received: 15 July 2016; Accepted: 9 October 2016; Published: 20 October 2016

**Abstract:** The LINER galaxy NGC 1052 is an ideal target to study the innermost regions of active galactic nuclei (AGN), given its close distance of about 20 Mpc. The source was observed at 29 epochs from 2005 to 2009 with the Very Long Baseline Array (VLBA) at 43 GHz. Here, we present a kinematic study of its twin-jet system from a subset of 9 epochs at 43 GHz carried out in 2005 and 2006, finding a bright central feature as the dynamic center. The resulting mean velocities of $\beta = v/c = 0.46 \pm 0.08$ and $\beta = 0.69 \pm 0.02$ for the western and eastern jet, respectively, give hints towards higher velocities in the eastern jet.

**Keywords:** galaxies: active; galaxies: nuclei; galaxies: jets; radio continuum: galaxies

## 1. Introduction

New developments and continuous improvements of current facilities make it possible to observe at short radio wavelengths of millimeters (mm) and sub-mm with dynamic ranges up to $10^3$, resulting in sensitivities of tens of $\mu$Jy/beam. This provides the opportunity to study the innermost regions in active galactic nuclei (AGN) at high angular resolution. The AGN in NGC 1052 has a luminosity distance of ∼21.7 Mpc, therefore 1 mas corresponds to ∼0.11 pc. NGC 1052 hosts a supermassive black hole (SMBH) with a mass of $\sim 10^{8.2}\,M_\odot$ [1] and is classified as a low-ionization nuclear emission-line region (LINER) [2–4]. Its double-sided jet system is oriented close to the plane of the sky, thus the bias due to Doppler boosting is tiny for the relatively low speeds observed in this source. Velocities of $\beta \sim 0.26$ have been reported [5,6]. A circumnuclear torus with a column density of $10^{22}\,\mathrm{cm}^{-2}$ to $10^{24}\,\mathrm{cm}^{-2}$ [6–8] covers large parts of the western jet. This leads to free-free absorption, which results in the occurrence of an emission gap between the two jet cores in radio images obtained with very-long-baseline interferometry (VLBI) up to 43 GHz. Given an optical depth of $\tau_{1\,\mathrm{GHz}} \sim 300$ to 1000 [8,9], its impact gets smaller toward higher frequencies, with only small absorption effects at 43 GHz and close to none at 86 GHz. Therefore, VLBI observations at mm wavelength peek through the absorbing structure and reveal the innermost regions around the central engine in NGC 1052.

The twin-jets were first detected at 86 GHz by [10]. In this work, we discuss a subset of a 43 GHz campaign carried out by the VLBA over 4 years, that reveals morphological similarities to the 86 GHz map. We present the dynamics of both jets at subparsec scales and discuss this in context of the jet morphology at 86 GHz.

## 2. Observation and Data Reduction

NGC 1052 was observed frequently during 2005 to 2009 at 43 GHz with the Very Long Baseline Array (VLBA). Standard calibration in AIPS with the implemented VLBA package was used to correct for residual errors in phase and amplitude. Maps have been produced in DIFMAP [11] using the CLEAN-algorithm and applying amplitude and phase self calibration iteratively. Two-dimensional Gaussian functions have been fitted to the visibility data.

We assumed an error on the position of the Gaussian components depending on the remaining noise in the clean and modelfit maps, the size of the components and the beam axis along the position angle (P.A.) of the jet .

$$\mathrm{d}\theta = \sqrt{\left(\frac{b_{\mathrm{paj}}}{(S/N)_{cm}}\right)^2 + \left(\frac{a_{\mathrm{paj}}}{(S/N)_{mm}}\right)^2}, \quad (1)$$

with $b_{\mathrm{paj}}$ the beam axis and $a_{\mathrm{paj}}$ the component axis along the jet P.A. of 64°. $(S/N)_{cm}$ is the signal-to-noise ratio of the map peak to the residual noise in the clean map and $(S/N)_{mm}$ is the signal-to-noise ratio of the component peak to the residual noise in the modelfit map. In the case of very small errors for small component sizes we set a lower boundary to the positional error of 1/10th the beam size [12].

## 3. Results

An excerpt of the 43 GHz CLEAN maps with Gaussian components overlaid is shown in Figure 1. In comparison to observations at lower frequencies, the maps reveal no significant emission gap, but one central, bright feature. There is a clear change in morphology when comparing the maps from 2005 and 2006 to those in 2007: in 2005 both jets emanate symmetrically to the north-east and south-west with an extent of about 4 mas. Starting in 2007 the structure becomes asymmetric. The eastern jet is shorter in comparison to the western one, in addition the overall structure is less extended. This can be a hint for internal asymmetries in the jet production.

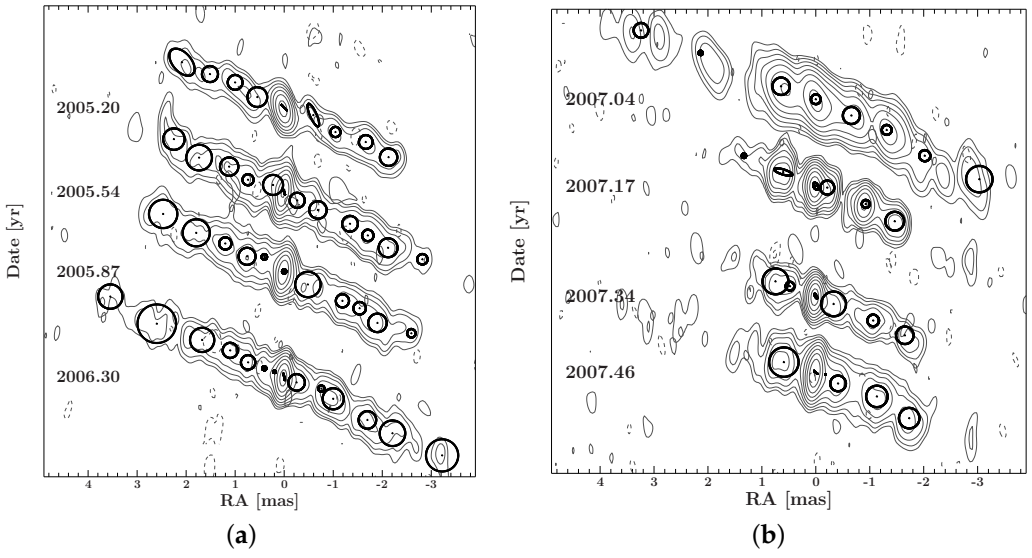


**Figure 1.** Selected clean maps of NGC 1052 from a 43 GHz campaign with the VLBA. The fitted two-dimensional Gaussian functions are plotted on top of the clean contours. (**a**): maps from 2005 showing highly symmetric jets, with one bright central feature; (**b**) maps from 2007; the jets are shorter and asymmetric. Map parameters are shown in Table 1. The contour lines begin at three times the noise level (see column 3 in Table 1) increase logarithmically by a factor of 2.

**Table 1.** Image parameters for all analyzed observations at 43 GHz with natural weighting. The RMS is taken from DIFMAP.

| Epoch | VLBA Code | RMS [mJy · beam$^{-1}$] | $S_{\mathrm{peak}}$ [Jy · beam$^{-1}$] | $S_{\mathrm{tot}}$ [Jy] | $b_{\mathrm{maj}}$ [mas] | $b_{\mathrm{min}}$ [mas] | PA [°] |
|---|---|---|---|---|---|---|---|
| (1) | (2) | (3) | (4) | (5) | (6) | (7) | (8) |
| 2005-03-11 | BR099A | 0.68 | 0.33 | 0.80 | 0.46 | 0.20 | 6.25 |
| 2005-07-18 | BR099D | 0.60 | 0.52 | 1.00 | 0.52 | 0.18 | −11.36 |
| 2005-11-13 | BR099G | 0.50 | 0.26 | 0.80 | 0.50 | 0.18 | −9.89 |
| 2006-04-09 | BR119B | 0.81 | 0.41 | 1.04 | 0.48 | 0.18 | −7.16 |
| 2007-01-14 | BR120A | 0.71 | 0.21 | 0.74 | 0.61 | 0.26 | 10.05 |
| 2007-03-04 | BR120B | 0.56 | 0.24 | 0.69 | 0.41 | 0.17 | −3.73 |
| 2007-05-05 | BR120C | 0.46 | 0.25 | 0.49 | 0.40 | 0.16 | −5.15 |
| 2007-06-17 | BR120D | 0.53 | 0.30 | 0.64 | 0.51 | 0.17 | −8.27 |

(1) date of VLBA observation, (2) VLBA experiment code; (3) rms noise level of image; (4) peak flux density; (5) total flux density; (6) FWHM major axis of restoring beam; (7) FWHM minor axis of restoring beam; (8) position angle of major axis of restoring beam.

Given the strong symmetry in the beginning of the 43 GHz campaign we analyzed the dynamics in the jet for the observations in 2005 and 2006. All maps show one prominent feature in-between both jets. To proceed on the assumption that this component is the center of both jet bases, all maps have been shifted such that its location is at the map origin. Because of the dominance in brightness and the compactness, this is the most likely choice. The Gaussian model components have been cross-identified by comparing between adjacent observations. This allowed us to apply linear fits to the trajectories for derivation of velocities in both jets (see Figure 2). We included errors on the component position $\theta$ in the least-square fits in accordance with Equation (1). Only components that could be tracked over at least 4 observations have been fitted. The components have been labeled starting with "ej" or "wj" for the eastern and western jet, respectively, and with numbers from 1 to 7 when going from the outer components to the inner ones.

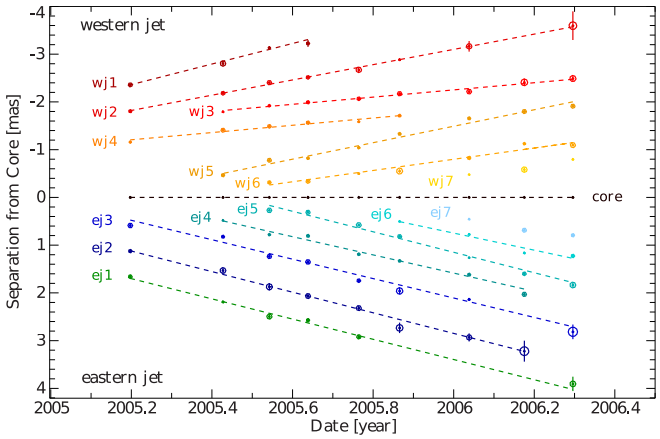


**Figure 2.** Component core-separation evolution for observations from 2005 and 2006.

From the linear fits, individual mean velocities for the western and eastern jet have been derived to be $\beta = 0.46 \pm 0.08$ and $\beta = 0.69 \pm 0.02$, respectively, giving a higher overall velocity for the eastern jet. Notice that the apparent velocities at 43 GHz are significantly higher than the $\beta \sim 0.26$ seen at lower frequencies [5,6].

## 4. Discussion

### *4.1. Dynamics in a Twin-Jet System*

The fits to the trajectories of the components in this twin-jet help us to understand the dynamics of the system. The velocities of single components in the jet flow are given by the slope of the linear

fit. The intersection of the line with the core position reveals the most likely date of ejection of a new component.

The differences in speed between eastern and western jet is clearly seen in Figure 3. Even though the western jet components follow different velocity systems, the western jet velocities are on the average clearly below these of the eastern jet. Given the differences in velocities in the western jet, the derived mean value is not a good representation. Instead it points out a change of the jet dynamics. This is not the case for the eastern jet, where all velocities have a spread of only 0.05 c around the mean value.

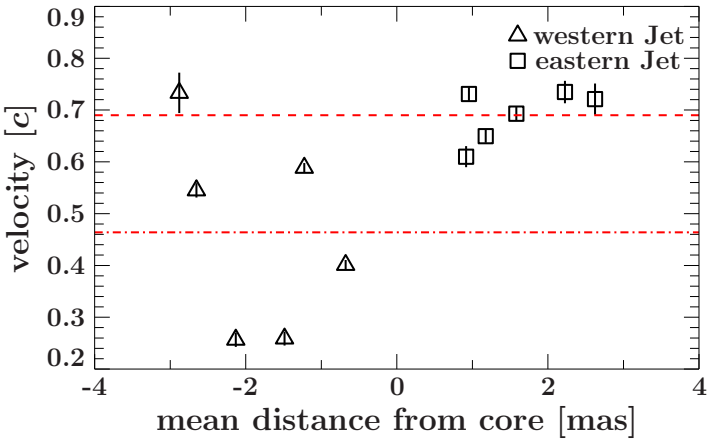


**Figure 3.** Velocity of tracked Gaussian components plotted over the mean separation of each trajectory from the center. The mean velocities are given by the dashed and dashed-dotted lines for the eastern and western jet respectively.

While the eastern jet components draw a consistent picture of the jet dynamics over time, the components in the western jet evolve in a different way. The components wj3 and wj4 are the slowest ones with $\beta \sim 0.27$ ; wj5 gets ejected with a faster velocity of $\beta \sim 0.59$ that is similar to wj2.

The ejection times of new components are not clearly synchronized (See Table 2 for the estimated component ejection dates). Only the components wj5 and ej4, as well as wj6 and ej5 are ejected at a similar time. All other component ejections seem not to be related to each other. The dynamics support the picture of asymmetric jets, as was already suggested based on the morphological changes. The difference in averaged velocities can be explained by intrinsic asymmetries in the jet dynamics. However, external absorption or disturbance is possible, too, but this is difficult to determine within the observations discussed herein.

**Table 2.** Ejection times of jet components ej1 to ej6 and wj1 to wj6. The errors on the ejection times are typically ∼0.1 years.

| Eastern jet | | Western jet | |
|---|---|---|---|
| **Component** | **Ejection Time [Year]** | **Component** | **Ejection Time [Year]** |
| **ej 1** | 2004.4 | **wj 1** | 2004.1 |
| **ej 2** | 2004.7 | **wj 2** | 2004.1 |
| **ej 3** | 2005.0 | **wj 3** | 2003.1 |
| **ej 4** | 2005.2 | **wj 4** | 2003.7 |
| **ej 5** | 2005.5 | **wj 5** | 2005.1 |
| **ej 6** | 2005.6 | **wj 6** | 2005.3 |

### *4.2. Comparison 86 GHz Image*

The central feature, which is the brightest over all observations, is likely the dynamic center of the source. That result has direct implications on the 86 GHz image, as the morphology is quite similar at both frequencies. Finding the dynamic center at one frequency defines the center at the other frequency, too. The stacked image of all 43 GHz observations between 2005 and 2009 results in a smooth map that can easily be compared to the tapered 86 GHz map. The maps at both frequencies are shown in Figure 4. In favour of an easy comparison, the tapered 86 GHz map has been convolved with the common beam from all 43 GHz images that had been used for the stacked image. Both maps show one central, bright peak, and clearly detect both jets, which have a smaller extent in the higher frequency image. The impacts of these findings are discussed in detail in [10], which leads to an upper limit on the distance of central engine to jet base of 100 Schwarzschild radii ($R_S$) and a magnetic field strength at 1 $R_S$ between 200 and $8.3 \times 10^4$ Gauss.

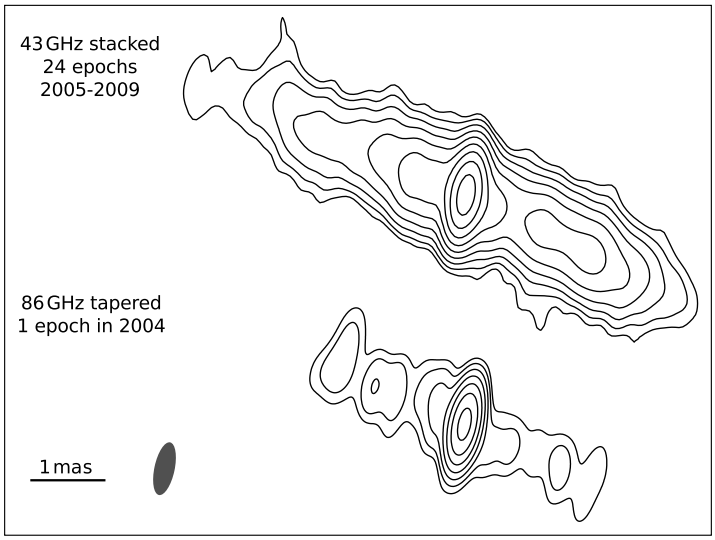


**Figure 4.** *Top*: stacked (multi-epoch) 43 GHz image; *Bottom*: tapered 86 GHz image, setting more weight to the shorter baselines. Both maps are restored with the common beam for all 24 analyzed 43 GHz epochs. Both maps show one central bright feature. Verifying this as the dynamic center at 43 GHz pinpoints the location of the central supermassive black hole (SMBH) at 86 GHz.

**Acknowledgments:** We acknowledge support and partial funding by the Deutsche Forschungsgemeinschaft grant WI 1860-10/1 and GRK 1147, the Spanish MINECO project AYA2012-38491-C02-01, AYA2013-4079-P, AYA2013-48226-C03-02-P, and AYA2015-63939-C2-2-P the Generalitat Valenciana projects PROMETEOII/2014/057, and PROMETEOII/2014/069. This research has made use of the software package ISIS [13] and a collection of ISIS scripts provided by the Karl Remeis Observatory, Bamberg, Germany at http://www.sternwarte.uni-erlangen.de/isis/, as well as an ISIS-DIFMAP fitting setup by C. Grossberger [14]. This research has made use of the NASA/IPAC Extragalactic Database (NED) which is operated by the Jet Propulsion Laboratory, California Institute of Technology, under contract with the National Aeronautics and Space Administration. This research has made use of data obtained with the Very Long Baseline Array (VLBA). The VLBA is an instrument of the National Radio Astronomy Observatory, a facility of the National Science Foundation operated under cooperative agreement by Associated Universities, Inc.

**Author Contributions:** Eduardo Ros and Matthias Kadler designed and performed the observations; Anne-Kathrin Baczko and Robert Schulz analyzed and interpreted the data; Manel Perucho contributed to the theoretical interpretation; All authors contributed in writing the paper.

**Conflicts of Interest:** The authors declare no conflict of interest.

## References

1. Woo, J.H.; Urry, C.M. Active galactic nucleus black hole masses and bolometric luminosities. *Astrophys. J.* **2002**, *579*, 530.

2. Fosbury, R.A.E.; Mebold, U.; Goss, W.M.; Dopita, M.A. The active elliptical galaxy NGC 1052. *Mon. Not. R. Astron. Soc.* **1978**, *183*, 549–568.
3. Ho, L.C.; Filippenko, A.V.; Sargent, W.L.W. A Search for "Dwarf" Seyfert Nuclei. III. Spectroscopic Parameters and Properties of the Host Galaxies. *Astrophys. J. Suppl.* **1997**, *112*, 315.
4. Mayall, N.U. The Occurrence of $\lambda$ 3727 [O II] in the Spectra of Extragalactic Nebulae. *Publ. Astron. Soc. Pac.* **1939**, *51*, 282–286.
5. Böck, M. Observations of Active Galactic Nuclei from Radio to Gamma-rays. Ph.D. Thesis, Friedrich-Alexander-Universität Erlangen-Nürnberg, Erlangen, Germany, 2012.
6. Vermeulen, R.C.; Ros, E.; Kellermann, K.I.; Cohen, M.H.; Zensus, J.A.; van Langevelde, H.J. The shroud around the twin radio jets in NGC 1052. *Astron. Astrophys.* **2003**, *401*, 113–127.
7. Kadler, M.; Ros, E.; Lobanov, A.P.; Falcke, H.; Zensus, J.A. The twin-jet system in NGC 1052: VLBI-scrutiny of the obscuring torus. *Astron. Astrophys.* **2004**, *426*, 481–493.
8. Kameno, S.; Sawada-Satoh, S.; Inoue, M.; Shen, Z.; Wajima, K. The Dense Plasma Torus around the Nucleus of an Active Galaxy NGC1052. *Publ. Astron. Soc. Jpn.* **2001**, *53*, 169–178.
9. Sawada-Satoh, S.; Kameno, S.; Nakamura, K.; Namikawa, D.; Shibata, K.M.; Inoue, M. Positional Coincidence of $H_2O$ Maser and a Plasma-Obscuring Torus in Radio Galaxy NGC 1052. *Astrophys. J.* **2008**, *680*, 191.
10. Baczko, A.-K.; Schulz, R.; Kadler, M.; Ros, E.; Perucho, M.; Krichbaum, T.P.; Böck, M.; Bremer, M.; Grossberger, C.; Lindqvist, M.; et al. A Highly Magnetized Twin-Jet Base Pinpoints a Supermassive Black Hole. *Astron. Astrophys.* **2016**, *593*, A47.
11. Shepherd, M.C.; Pearson, T.J.; Taylor, G.B. *Bulletin of the American Astronomical Society*; American Astronomical Society (AAS): Washington, DC, USA; 1994; Volume 26, p. 987.
12. Lister, M.L.; Cohen, M.H.; Homan, D.C.; Kadler, M.; Kellermann, K.I.; Kovalev, Y.Y.; Ros, E.; Savolainen, T.; Zensus, J.A. MOJAVE: monitoring of jets in active galactic nuclei with VLBA experiments. VI. Kinematics analysis of a complete sample of blazar jets. *Astron. J.* **2009**, *138*, 1874.
13. Houck, J.C.; Denicola, L.A. *Astronomical Data Analysis Software and Systems IX*; Manset, N., Veillet, C., Crabtree, D., Eds.; Astronomical Society of the Pacific Conference Series; Astronomical Society of the Pacific: San Francisco, CA, USA, 2000; Volume 216, p. 591.
14. Grossberger, C. New Developments and Techniques in Radio to X-ray Observations of AGN. Ph.D. Thesis, Friedrich-Alexander-Universität Erlangen-Nürnberg, Erlangen, Germany, 2014.